JOURNAL OF AGRICULTURAL AND FOOD CHEMISTRY

Article

pubs.acs.org/JAFC

Dual Effects of Chitosan Decoration on the Liposomal Membrane Physicochemical Properties As Affected by Chitosan Concentration and Molecular Conformation

Chen Tan, Jin Xue, Karangwa Eric, Biao Feng, Xiaoming Zhang, and Shuqin Xia*

State Key Laboratory of Food Science and Technology, School of Food Science and Technology, Jiangnan University, Lihu Road 1800, Wuxi, Jiangsu 214122, China

ABSTRACT: This study was devoted to a further understanding of the dependence of liposomal membrane properties on chitosan conformation and proved the dual effects of chitosan. The concentration dependence of chitosan conformation in aqueous solution was illustrated by surface tension and fluorescence probe techniques. Fluorescence and Raman spectra were subsequently employed to investigate the dynamic and structural changes of the liposomal membrane resulting from chitosan decoration. Results showed that the unfolded and crimped chains of chitosan flatly adsorbed onto the membrane surface via electrostatic attraction and favored liposome stability. Furthermore, the adsorption of crimped chains seemed stronger due to the embedding of their hydrophobic moieties. However, the presence of chitosan coils induced the increase in membrane fluidity, the intrachain disorder in lipid molecules, and the *gauche* conformation change of choline group. Dynamic light scattering and lipid oxidation measurements demonstrated that this perturbation was correlated with the permeation of coils into the lipid bilayer.

KEYWORDS: *chitosan conformation, dual effects, liposome, stability, perturbation*

INTRODUCTION

Liposomes are colloidal systems where phospholipids were dispersed in aqueous solution followed by forming the bilayer membrane of vesicles through self-assembling. They have long been studied as efficient drug and nutraceutical delivery systems because of their ability to carry hydrophobic and hydrophilic drugs.[1,2] Despite that, liposome stability *in vitro* and *in vivo* remains a setback, due to their high tendency to degrade or aggregate and fuse leading to leakage of the entrapped compounds during storage or after administration.[3] To overcome those problems, liposome surfaces have been modified with polymers and adapted to the environment of application, thus achieving higher performance. Natural polymers have received special attention because of their use in decorating and improving liposome characteristics. Among them, chitosan produced by the deacetylation of chitin, has shown many advantages due to its biocompatibility, biodegradability, and low toxicity.[4] Investigations of the chitosan−liposome system for the past decade have mainly focused on the following factors: various environmental stresses (pH and salt concentration),[5] the lipid bilayer properties (lipid chemical structure and configuration),[6,7] and chitosan characteristics (molecular weight, deacetylation degree, and solution concentration).[8,9] It is generally accepted that chitosan decoration via electrostatic attraction can improve the liposomes structural properties, biocompatibility, and drug (or nutraceutical) delivery efficiency.[10,11] Nevertheless, some studies found negative effects of chitosan decoration on liposome properties. For instance, Fourier transform (FT)−Raman spectroscopy has demonstrated that chitosan directly perturbed the organizations of the hydrophobic inner core of the dipalmitoyl-*sn*-glycero-3-phosphocholine (DPPC) bilayer.[12] Through Langmuir monolayers, it proved that chitosan can show a disrupting effect on the phospholipid membranes.[13] Chitosan can also act as a bioadhesive and permeabilizer when protonated (pH < 6.5), making it an ideal candidate for mucosal drug delivery.[14] However, this effect of adsorption enhancement may in turn cause a potential damage to liposomal membrane integrity and stabilization. The contradiction in these reports shows that the mechanisms of chitosan action are still debatable, proving that broader research is needed to further understand the dual effects of chitosan decoration.

Previous studies have already demonstrated that the permeabilizing and perturbating effects of chitosan on the liposomal membrane can be controlled by pH, molecular size, and concentration.[12,15] As these parameters seemed to be partially associated with the conformational change, one probable direction to find out the reasons for the chitosan dual effects was to understand the roles of chitosan conformation. Polyelectrolyte conformation can affect its organization and adsorption behaviors onto the liposome surface. For instance, it was suggested that at very low degrees of coverage, polyelectrolyte chains have a tendency to flatten, while at higher degrees of coverage, they gradually may form coils and trains.[16] The adsorption behaviors further affected the membrane properties, including fusion, aggregation and disruption behavior,[17,18] permeability,[19] and phase transformations.[20] Interestingly, recent studies have suggested that chitosan displayed more surface activities when the concentration exceeded its critical aggregation concentration (CAC) and behaved more like a Gaussian coil instead of the wormlike chain model by intra-and inter molecules hydrophobic interactions.[21,22] These findings concentrating on the con-

Received: April 10, 2013
Revised: June 13, 2013
Accepted: June 17, 2013
Published: June 17, 2013

dx.doi.org/10.1021/jf401556u | J. Agric. Food Chem. 2013, 61, 6901−6910

formational variation of chitosan in aqueous solution may guide the mechanism research of chitosan dual effects. This was the reason why, in the present article, we first focused on the concentration dependence of chitosan conformation, followed by its influence on membrane properties. Unfortunately, most reports used very low chitosan concentrations (below CAC) to decorate liposomes and demonstrated the positive effects. When the polymer chains of chitosan were well extended, their binding on the membrane surface was considered as a flat adsorption.[6] Thus, we speculated that some other probable adsorption behaviors of chitosan with regard to its conformations resulted in the dual effects on the membrane, which seemed of much interest to investigate.

However, in order to understand and probe the adsorption mechanism, one has to consider the physical properties of the polymer as well as the interactions with membrane. Different organizations of the polyelectrolyte on the vesicles suggested that different types of interactions may be involved. Of course, electrostatic interaction was considered as the main energy contribution in charged chitosan-decorated liposomes. A progressive decrease of the vesicle net charge can be observed with the adsorption of chitosan, followed by the charge inversion and appearance of overcharging effect.[23] Besides electrostatics, hydrophobic interaction may be also involved, which probably appeared between phospholipid apolar tails and the polymer backbone.[24] Some other interactions such as hydrogen bonding and van der Walls forces have also been inferred in the literature via the Langmuir monolayer model.[25]

The further understanding of the relationship between liposomal membrane properties and adsorption of chitosan with varying conformations will be crucial for the development of drug and nutraceutical delivery systems. Herein, the conformational change of chitosan in aqueous solution as a function of its concentration was investigated by a combination of surface tension technique and fluorescence probe 1,6-diphenyl-1, 3, 5-hexatriene (DPH). Then, the changes in the liposomes' dynamic and structural properties resulting from their interactions with chitosan of varying conformations were analyzed by fluorescence and Raman spectra. The particle size and ζ potential were applied to trace the vesicles state upon chitosan adsorption. Lipid peroxidation measurements were also introduced to reflect the chitosan-induced perturbation effect on the liposomal membrane. On the basis of the experimental results, the probable models for the adsorption behavior and structural organization of chitosan on the liposomal bilayer membrane were proposed.

MATERIALS AND METHODS

Materials. Egg yolk phospholipid (EPL) was purchased from Chemical Reagent Plant of East China Normal University (Shanghai, China). Polyoxyethylene sorbitan monooleate (Tween 80) was obtained from China Medicine (Group) Shanghai Chemical Reagent Co. (Shanghai, China). The fluorescent probe 1,6-diphenyl-1,3,5-hexatriene (DPH, 98% pure) was purchased from Sigma-Aldrich. Partially deacetylated chitosan (85%) with average molecular weight of 200,000 was purchased from Ao Xing Biotechnology Co., Ltd. (Zhejiang, China). All other reagents were of analytical grade.

Preparation of Bare Liposomes and Chitosan-Decorated Liposomes. Bare liposomes were prepared according to our earlier method with a slight modification.[26] Phospholipid (6 g) and Tween 80 (4.32 g) were dissolved in 12 mL of warm ethanol at 55 °C. The ethanol solution was rapidly injected using a syringe as a pump into 120 mL of buffer solution (0.1 M acetic acid/0.01 M phosphate, 75 mM NaCl, pH 4.0) at 55 °C in a water bath under stirring at 700 r/min using an IKA RW 20 digital overhead stirrer (IKA Works Guangzhou). The aqueous phase immediately became milky as a result of liposome formation. After agitation for 30 min, the liposomal system was transferred to a round-bottom flask attached to a rotary evaporator at 55 °C and reduced pressure to remove ethanol. The obtained liposomal suspension was then submitted to a probing sonication process in an ice bath for 10 min at 240 W with a sequence of 1 s of sonication and 1 s rest using a sonicator (Sonics & Materials, Inc., 20 kHz). The final samples were filled into vials (the headspace of the vials was blanketed with nitrogen) and kept in the refrigerator (about 4 °C in the dark).

The chitosan-decorated liposomes were prepared using the methods described by Henriksen et al.[27] The chitosan was dissolved in the same buffer solution for bare liposomes and then added dropwise to a bare liposomal suspension at equal volume at 1000 r/min for 30 min using an overhead stirrer. The final concentration of chitosan was adjusted from 1 to 4 mg/mL. The phospholipid concentration in final samples was kept at 25 mg/mL. The decorated liposomes were filled into vials and stored at the same conditions as bare liposomes.

Surface Tension Analysis. Chitosan was dissolved in buffer solution (0.1 M acetic acid/0.01 M phosphate and 75 mM NaCl, pH 4.0) with concentrations ranging from 0.1 to 5 mg/mL. The surface tension measurements of chitosan in buffer solution were tested with the Wilhelmy plate method with a digital tensiometer (DCAT21, Dataphysics, Germany) at room temperature. The surface tension values as a function of chitosan concentration were determined, and the readings were fixed until the standard deviation was lower than 0.030 mN/m.

Fluorescence Intensity and Microviscosity Measurements. The DPH stock solution was prepared according to our previous studies.[28] Briefly, small amounts of DPH powders were weighted and dissolved in tetrahydrofuran. The final concentration of DPH was adjusted to 2×10^{-3} mol/L. The stock solution was kept at 4 °C in the dark. When using, aliquots of 250 μL of DPH stock solution was added to the 25 mL volumetric flask and diluted with buffer solution (0.1 M acetic acid/0.01 M phosphate, 75 mM NaCl, pH = 4.0). The final concentration of DPH was adjusted to 2×10^{-5} mol/L.

For chitosan solutions, a small quantity of the above diluted DPH stock solution was added to the chitosan solution to give a final concentration ranging from 0.1 to 5 mg/mL, followed by incubating at 37 °C for 1 h. The pH was maintained at 4.0 with acetic acid or NaOH adjustment when required.

For liposome suspensions, aliquots of DPH solution were first mixed with bare liposomes in a 10 mL tube, incubating at 37 °C for 1 h. Then the chitosan of different concentration in the same buffer was added dropwise to the incubated sample under stirring at 1000 r/min for 30 min. The final lipid/probe molar ratio was 1000:1.

Fluorescence intensity and fluorescence depolarization were excited at 360 nm, and emission was recorded at 450 nm with a spectrofluorimeter (Hitachi F-7000, Japan). The excitation and emission slit width were both fixed at 5 nm. The fluorescence depolarization was measured as the following protocol. The samples were excited first by vertical polarized light, two polarizing parts of horizontal $I_{0,0}$ and vertical $I_{0,90}$ were obtained. Then, the samples were excited by horizontal light, two polarizing parts of horizontal $I_{90,0}$ and vertical $I_{90,90}$ were recorded. The microviscosity (η) of the environment surrounding DPH was calculated from the following equation:[29]

$$\eta = \frac{2P}{0.46 - P}$$

where P was the fluorescence polarization, $P = (I_{0,0} - GI_{0,90})/(I_{0,0} + GI_{0,90})$; G was the grating correction coefficient, $G = I_{90,0}/I_{90,90}$.

Raman Spectra Analysis. Raman spectra were recorded using a portable laser Raman spectrometer (RamTracer-200-WF-B, Opto-Trace Technologies, Inc., USA) equipped with a 785 nm near-infrared frequency stabilized laser source. The laser output power was 334 mW, and the collection time was 20 s. The Raman samples (bare liposomes and chitosan-decorated liposomes) were prepared as described above. An ordinary Raman spectrum was baseline-corrected, and the Raman

intensities were measured as peak height. The Raman spectrum was collected in the ranges of 600−1200 and 2800−3000 cm^{-1}. The order parameters (I_{714} cm^{-1}/I_{1330} cm^{-1}, I_{1124} cm^{-1}/I_{1084} cm^{-1}, I_{2884} cm^{-1}/I_{2850} cm^{-1}, and I_{2884} cm^{-1}/I_{2930} cm^{-1}) were the intensity ratio of the two bands and were deduced from Raman spectra.

Particle Size and ζ Potential Determination. Measurements were performed at (25 ± 0.1)°C using a commercial zeta-sizer (Nano-ZS90, Malvern Instruments Ltd., United Kingdom) with a He/Ne laser (λ = 633 nm) anda scattering angle of 90°. Aliquots of 1 mL liposomal dispersion were diluted to 10 mL with the same buffer solution to avoid multiple scattering phenomena due to interparticle interaction. Immediately, the diluted sample was transferred into the polystyrene cuvette for size determination or capillary cells for zeta potential (ζ), and then the z-average diameter (D_z) and particle size distribution (polydispersity index, PDI) were recorded by dynamic light scattering (DLS). The measured mobility u is transformed into ζ-potential according to the Smouluchowski relationship $\zeta = u\eta/\varepsilon$, where η and ε are the viscosity and permittivity of the solution, respectively.[30] The measurements were repeated three times, and the results given are the average values.

Determination of Malonaldehyde (MDA) Value. MDA, a final product of fatty acid peroxidation, reacted with TBA to form a colored complex that had a maximum absorbance at 535 nm. The MDA concentration was determined spectrophotometrically by the thiobarbituric acid (TBA) reaction following the method of earlier studies.[31] A solution containing TBA (15%, w/v), trichloroacetic acid (0.37%, w/v), and hydrochloric acid (1.8%, v/v) was added to 1 mL of liposomal sample and mixed followed by heating at 100 °C for 30 min. Afterward, the mixture was cooled rapidly with an ice bath, centrifuged for 5 min at 2000 r/min, and filtrated. The absorbance of the filtrate was measured by a spectrophotometer at 535 nm ($A_{535\ nm}$). The determination of malonaldehyde (MDA) was calculated using the following equation:

$$\text{MDA (ng/mL)} = \frac{A_{535nm} \times 4.15 \times 1000}{W}$$

where 4.15 is the conversion coefficient of milliliter liposomes containing malonaldehyde, μg/mL; W is the lipid content per volume, mg/mL.

RESULTS AND DISCUSSION

Aggregation of Chitosan in Aqueous Solution. Chitosan, the molecular conformation more like a single-stranded worm, is commonly regarded as a polymer with low surface activity. However, an aggregation behavior in aqueous solution has been found in some reports by static light scattering[32] and pyrene fluorescence.[33] It has been suggested that the aggregation behavior was mainly concentration and molecular weight dependent.

Figure 1 showed that the surface tension at chitosan concentrations of 1.0 mg/mL or lower was similar to the value observed in bulk phase. The almost constant values indicated that chitosan molecules were excluded from the air/solution interface, thus suggesting the absence of surface activity within the studied concentration range. With further increase of the chitosan concentration from 1.0 to 3.5 mg/mL, surface tension decreased continuously. This phenomenon may be explained by the adsorption of hydrophobic moieties in chitosan molecules, at least partially, on the air/solution interface. The hydrophobic character along the chitosan chain becomes stronger, and thus, the chitosan self-aggregates appeared in buffer solutions by intra- and intermolecular hydrophobic interactions.[22] This concentration at which chitosan starts aggregating was similar to the finding in a previous study.[21] However, some researchers[34] reported that the surface tension of chitosan solutions ranging from 0 to 4

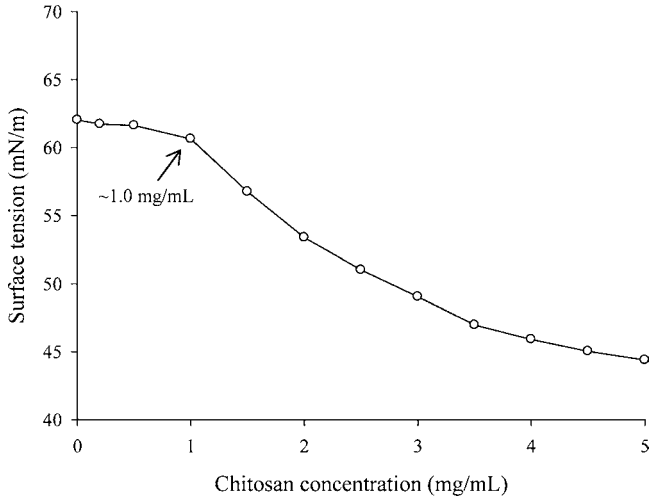

Figure 1. Concentration dependence of the surface tension for chitosan in aqueous solution (0.1 M acetic acid/0.01 M phosphate and 75 mM NaCl, pH 4.0) at 25 °C.

mg/mL was the same as that of pure water, and structural parameters of the polymer did not have any effect over this property. The contradiction in the literature with regard to the surface activity of chitosan was elucidated by the group of Pavinatto,[35] who claimed that the main reasons may be related to the difference of chitosan characterization including the molecular weight, deacetylated degree, ionization degree of the amine group, and the viscous effects for increasingly concentrated chitosan.

DPH is a rigid bar small molecule which has a strong lipophilicity and is expected to localize preferentially in the hydrophobic domains of amphipathic molecules. Its fluorescence emission spectrum is very sensitive to the polarity of the surrounding environment.[36] The lower the polarity of microenvironment, the higher is the fluorescence intensity. Figure 2 showed that the fluorescence intensity of DPH in chitosan solution below 1.0 mg/mL was close to the value in bulk solution based on the practically constant value of F/F_0. It implied that DPH still located in the polar environment and that the molecular chain of chitosan was well extended at this low concentration range. The increase of chitosan concentration from 1 to 3.5 mg/mL induced a significant increase of F/F_0. As demonstrated above, when increasing the chitosan concentration, the hydrophobic character along the chitosan chain became stronger, and then the intra- and inter-hydrogen bonding and hydrophobic interactions between the chains may exert a greater influence on the conformation of chitosan molecular chain. Thus, it was believed that the increased F/F_0 indicating the decreased polarity of the environment surrounding DPH was due to the formation of some hydrophobic microdomains by chitosan molecules that DPH could occupy. Similar trends were also observed by Li,[37] who gave the explanation that chitosan chains turned, were crimped, and formed the irregular coil structures in aqueous solution when concentration were above 1 mg/mL.

Figure 2 also presents the microviscosity of the environment surrounding DPH. At low chitosan concentrations ranging from 0 to 1 mg/mL, a significant increase of η/η_0 was observed. Taking into account the constant values of fluorescence intensity, it was clear that the increase of microviscosity was mainly due to the increase of solution viscosity with chitosan

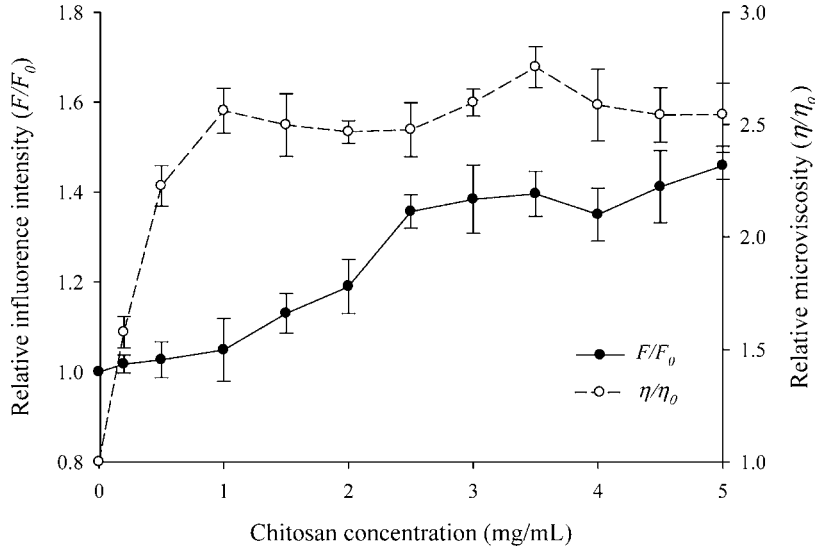

Figure 2. Relative fluorescence intensity (F/F_0) and microviscosity (η/η_0) in chitosan aqueous solution (0.1 M acetic acid/0.01 M phosphate and 75 mM NaCl, pH 4.0) as a function of chitosan concentration. F_0 and η_0 refer to the DPH fluorescence intensity and calculated microviscosity in buffer solution without chitosan, respectively; F and η refer to the DPH fluorescence intensity and microviscosity in the same buffer solution containing chitosan. Each data point is expressed as the mean value ± standard deviation (n = 3).

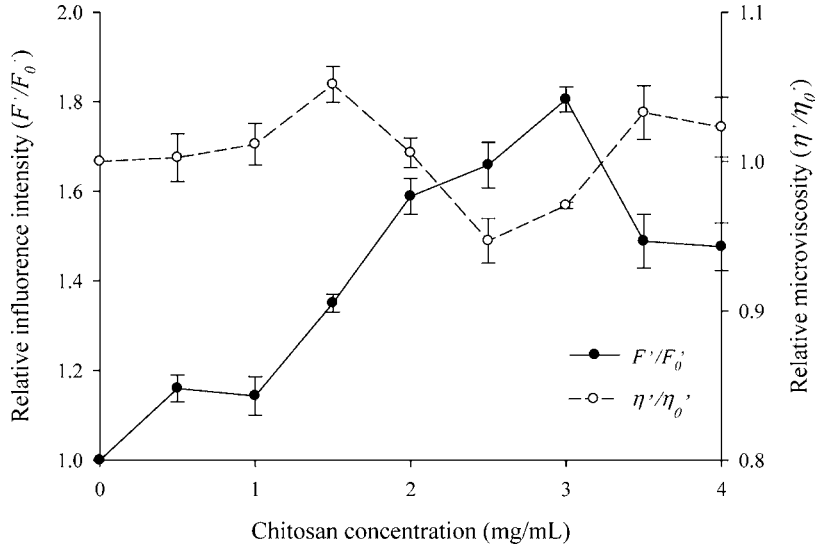

Figure 3. Relative fluorescence intensity (F'/F_0') and microviscosity (η'/η_0') in liposomes as a function of decorated chitosan concentration. F_0' and η_0' refer to the DPH fluorescence intensity and calculated microviscosity in bare liposomes, respectively; F' and η' refer to the DPH fluorescence intensity and microviscosity in chitosan-decorated liposomes, respectively. Each point represents the mean value ± standard deviation (n = 3).

addition. From 1 to 2 mg/mL, η/η_0 values were almost unchanged. The probable reason was that the inside of these formed microdomains where DPH was present still exhibited polar properties. When progressively increasing the concentrations from 2 to 3.5 mg/mL, we obeserved that the microviscosity increased along with the relative fluorescence intensity. Within this range, a higher percentage of crimped molecular chains turned into irregular coils followed by the generation of more hydrophobic microdomains. Furthermore, excessive irregular coils began associating with each other and formed packed coils, thereby leading to the microviscosity increase around DPH.

On the basis of the data of surface activity and fluorescent measurements, it was believed that the aggregates of chitosan molecules started to appear from 1 mg/mL. Furthermore, this self-aggregation behavior was considered to be the driving force for the conformational change of chitosan. It seemed that there existed at least four main conformations, including unfolded chain, crimped chain, irregular coil, and packed coil. As expected, these determined structures were helpful in investigating the dependence of liposome physiochemical properties upon chitosan conformation, which are discussed in the following sections.

Effect of Chitosan Decoration on Liposomal Membrane Fluidity. The stability of liposomes is closely related to the fluidity of the liposomal membrane, which quantificationally characterizes the mobility and molecular rotation rate of the lipid.[38] The fluorescence probe DPH is widely used for measuring the order of the lipid fatty acyl chains in the core region of the bilayer due to its hydrophobic properties. To reflect the influence of the chitosan conformation on membrane fluidity, relative fluorescence intensity (F'/F_0') and

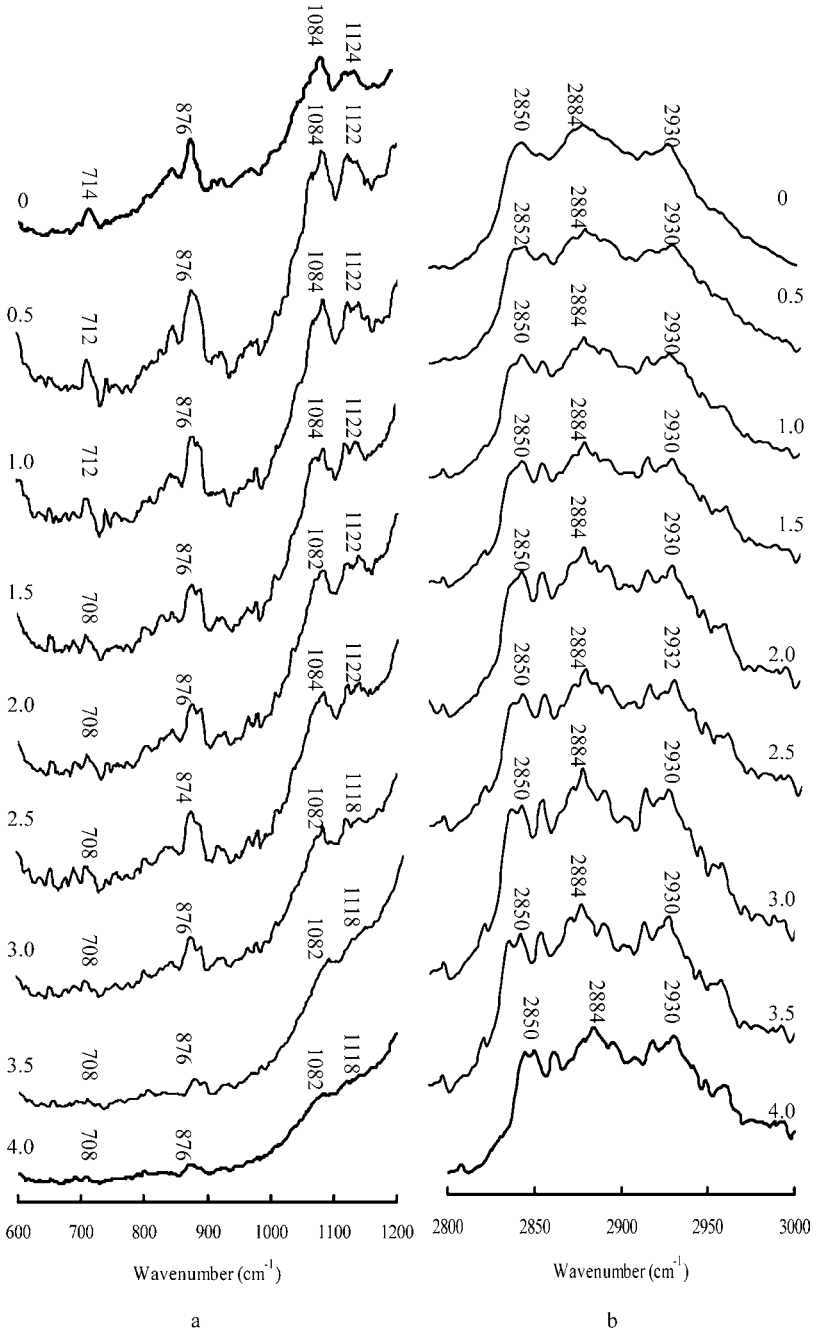

Figure 4. Raman spectra of liposomes containing different chitosan concentrations in the range from 600 to 1200 cm^{-1} (a) and 2800 to 3000 cm^{-1} (b).

microviscosity (η'/η_0') surrounding DPH in chitosan-decorated liposomes were determined.

As Figure 3 shows, F'/F_0' increased continuously with increasing chitosan concentration from 0 to 3.0 mg/mL. As the added amounts of DPH were constant, it meant that the higher the addition of chitosan, the more the DPH molecules incorporated in the liposomal bilayer. This result was believed to correlate with the formation of more hydrophobic microdomains by the insertion of hydrophobic moieties of chitosan into the liposomal membrane. However, F'/F_0' decreased when chitosan concentration exceeded 3.0 mg/mL, suggesting that some percentage of DPH leaked from the lipid bilayer into the aqueous solution. The leakage may be explained by the penetration of excessive chitosan into the membrane bilayer, followed by promoting a disturbance and disruption of bilayer organization.

The relative microviscosity η'/η_0' in Figure 3 shows that the membrane fluidity of the decorated liposome was lower than that of bare liposomes and progressively decreased when the chitosan concentration increased from 0 to 1.5 mg/mL. Chitosan was in the form of unfolded and crimped chains at this stage. Thus, it was clear that the higher the chitosan linear chain adsorption, the lower is the membrane fluidity. However, the further increase of chitosan concentrations from 1.5 to 2.5 mg/mL was accompanied by the enhancement of liposomal membrane fluidity. Note that the irregular and packed coils generated by the intensified self-aggregation is above 1.5 mg/mL, that is, the presence of these coils contributed to the

dx.doi.org/10.1021/jf401556u | J. Agric. Food Chem. 2013, 61, 6901−6910

increment of membrane fluidity. Figure 3 also presented an interesting phenomenon that the microviscosity increased at very high chitosan concentrations. This might be due to the fact that part of the DPH leaking out from the liposome bilayer incorporated into the hydrophobic microdomains of chitosan random coils.

Raman Spectroscopy Analysis. The polar group of a lipid bilayer was the interaction site of foreign charged molecules, which could change the physicochemical properties of the lipid bilayers. Therefore, the choline group, the part of the polar head, was appropriate to analyze the change of interfacial region of the membrane induced by the interaction of chitosan molecules. The backbone of the choline group (O-C-C-N^+) mostly takes on the *gauche* conformation around the C−C bond in the bilayers. Hauser et al.[39] reported that a structural change from the *gauche* to the *trans* conformation in the choline groups took place in the presence of charged ions. The *gauche* conformation of the O-C-C-N^+ backbone gave a band in the region from 710 to 720 cm^{-1}, while the *trans* conformation did at about 770 cm^{-1}. Figure 4a showed the Raman spectra of bare and chitosan-decorated liposomes in the region from 600 to 1200 cm^{-1}. A relatively strong band at around 714 cm^{-1} in bare liposomes was observed, while no band at around 770 cm^{-1} appeared. It indicated that most of the choline groups took on the *gauche* conformation in the liposomal bilayer. To present the variation of *gauche* conformation quantitatively as a function of chitosan concentration, the CH_2 twisting vibration of hydrocarbon chains near 1330 cm^{-1} was used as an internal standard.[40] This band was sensitive to the state of the hydrocarbon chains but was relatively insensitive to the conformation of the polar headgroup. As shown in Table 1, the ratio of the band at 714 cm^{-1} to that at 1300 cm^{-1} (I_{714}/I_{1330}) almost unchanged with the addition of chitosan from 0 to 1.5 mg/mL. Only a small peak shift was observed from 714 cm^{-1} to 708 cm^{-1}. It implied that the adsorption of chitosan on liposomes as a form of unfolded and crimped chain did not induce an obvious structural change of the *gauche* conformation in the choline group. By contrast, a dramatic decrease of the ratio was observed at concentrations above 1.5 mg/mL. Figure 4a also evidenced that intensity of the peak at around 708 cm^{-1} decreased from 1.5 mg/mL, even almost disappearing from 3.5 mg/mL. Taking into account the conformation of chitosan in this concentration range, it can be concluded that the presence of chitosan coils induced some degree of *gauche* conformation change. Another phenomenon should also be noted that no obvious peak was detected at 770 cm^{-1}, indicating no great structural change from the *gauche* to the *trans* conformation.

Table 1. Order Parameters of Liposomes Containing Different Concentrations of Chitosan As Deduced from Raman Spectra

chitosan concn (mg/mL)	I_{714} (cm^{-1}) /I_{1300} (cm^{-1})	I_{1124} (cm^{-1}) /I_{1084} (cm^{-1})	I_{2884} (cm^{-1}) /I_{2850} (cm^{-1})	I_{2884} (cm^{-1}) /I_{2930} (cm^{-1})
0	0.60	0.97	1.05	1.05
0.5	0.66	0.99	1.04	1.04
1.0	0.66	0.99	1.04	1.04
1.5	0.60	1.00	1.04	1.04
2.0	0.56	1.00	1.04	1.03
2.5	0.54	1.00	1.04	1.02
3.0	0.49	1.00	1.04	1.01
3.5	0.34	1.00	1.04	1.01
4.0	0.27	1.00	1.04	1.01

The C−C stretching mode at 1130 cm^{-1} was associated with chains in the *all-trans* conformation, while the feature at 1100 cm^{-1} was associated with hydrocarbon chains containing *gauche* rotations.[41] The ratio I_{1124}/I_{1084} could quantitatively measure the number of phospholipid hydrocarbon chain segments in the *all-trans* conformation and *gauche* rotation, reflecting the degree of the longitudinal order of liposomes.[42] As shown in Table 1, adsorption of chitosan only led to a slight increase of I_{1124}/I_{1084} of bare liposomes, suggesting an increase of *gauche*/*trans* population and the longitudinal order of liposomes. However, the I_{1124}/I_{1084} variation in chitosan-decorated liposomes was not significantly altered regardless of the chitosan concentrations.

The bands located at about 2850 cm^{-1}, 2890 cm^{-1}, and 2930 cm^{-1} were derived from the methylene C−H symmetric stretching, the methylene C−H antisymmetric stretching, and the Fermi interaction of the methylene groups with the terminal methyl group, respectively.[43] Figure 4b shows the Raman spectra of the bare and chitosan-decorated liposomes from 2800 to 3000 cm^{-1}. The I_{2884}/I_{2850} intensity ratio of bare and chitosan-decorated liposomes was similar to each other, as summarized in Table 1. The I_{2884}/I_{2850} responds to the changes in both the lateral packing of the chains and the *trans*−*gauche* population ratio.[44] The practically unchanged values suggested that chitosan adsorption exerted very weak influence on the lipid chain lateral packing. The I_{2884}/I_{2930} was widely used for elucidating the intramolecular conformation of the acyl chains in the bilayer, and a decrease of the ratio indicated an increase of intrachain disorder in lipid membrane. The I_{2884}/I_{2930} of chitosan-decorated liposomes was similar to that of bare liposomes, and its variation seemed independent of the chitosan concentration ranging from 0.5 to 1.5 mg/mL. It indicated that the adsorption of the linear chain (unfolded or crimped chain) exerted no influence on intrachain organization in the membrane. However, intrachain disorder appeared from 2.0 mg/mL, which may be explained by the interactions of the chitosan coil with the lipid bilayer.

Effect of Chitosan Decoration on the Liposomal Size and Charge. To understand the organization of chitosan chains on the liposome surface and associated interaction mechanisms, the liposomal size and ζ potential were employed to trace the vesicles state during chitosan titration. The average diameter (D_z) of bare liposomes was 82.98 ± 1.42 nm with a negative charge (−17.9 ± 1.0 mV), as shown in Figure 5. After titration with chitosan to get the final concentration of 0.5 mg/mL, D_z increased to 90.14 ± 1.05 nm, and the ζ potential value was measured to be +10.6 ± 0.7 mV. The diameter increase and charge inversion were understandable because of the adsorption of positively charged polymer chains onto the negative region of the liposome surface. D_z and positive potential values progressively increased with more chitosan addition until 2.0 mg/mL. Nevertheless, an unexpected phenomenon appeared causing D_z to suddenly decrease ranging from 2.0 to 4.0 mg/mL accompanied by a potential plateau in large excess of chitosan. These behaviors may be correlated with the formation of chitosan random coils and their interactions with lipid bilayers, as discussed further. Analysis of the size distribution (Figure 5b) showed that although an increase appeared at the initial titration process (below 2.0 mg/mL), the PDI values remained lower than 0.3 indicating a relatively homogeneous dispersion.[45] With more chitosan addition, however, the values increased dramatically, even

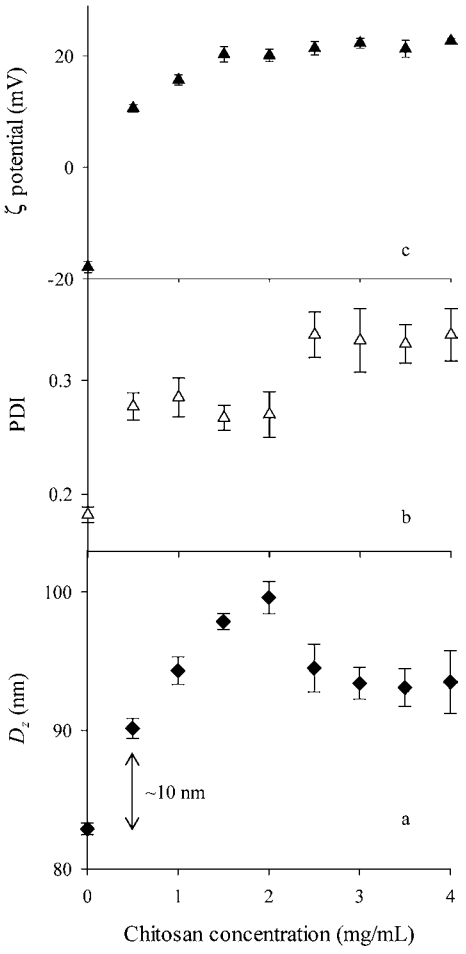

Figure 5. *z*-Average diameter (D_z) (a), size distribution (polydispersity index, PDI) (b), and ζ potential (c) of liposomes with chitosan decoration. Each data point was expressed as the mean value ± standard deviation (n = 3). The arrow in panel a refers to the thickness of the chitosan layer at the initial titration, indicating a flat adsorption.

reached approximately 0.340 at 4.0 mg/mL. Figure 6 presents the diameter distribution of bare and decorated liposomes containing low concentrations of chitosan (because their distributions were almost the same, only chitosan-decorated liposomes at 2.0 mg/mL were given), demonstrating that they only had a sharp peak, contrary to the two strong volume peaks obviously found above 2.5 mg/mL. This size distribution corresponded well with the PDI results. Note that the peak of decorated liposomes at 2.5 mg/mL located in the range of 10 to 50 nm became stronger compared with that at 4.0 mg/mL. The decrease of particle diameter implies that the liposomal vesicles underwent a certain degree of disruption resulting from the coil formation of chitosan.

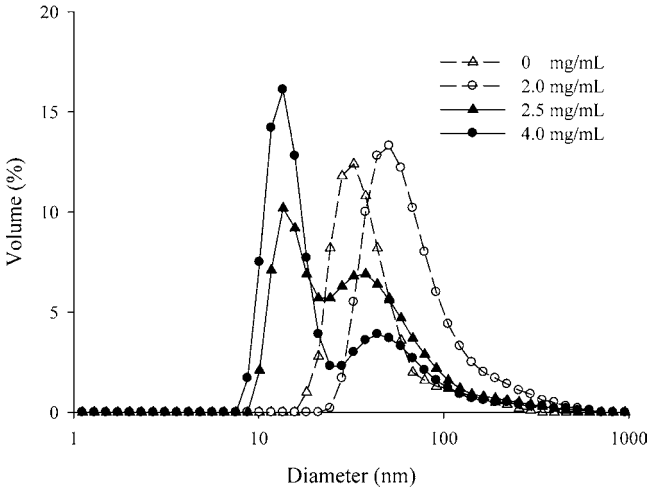

Figure 6. Diameter distribution of liposomes before and after decoration with different concentrations of chitosan (2.0, 2.5, and 4.0 mg/mL).

Effect of Chitosan Decoration on Lipid Oxidation of Liposomes. The dynamic and structural change of the lipid bilayer was believed to affect membrane permeability, which can be indirectly evaluated by lipid oxidation.[46] Thus, the amounts of malonaldehyde (MDA) generated from lipid oxidation were measured during storage, and the results are shown in Figure 7. Bare liposomes exhibited serious lipid

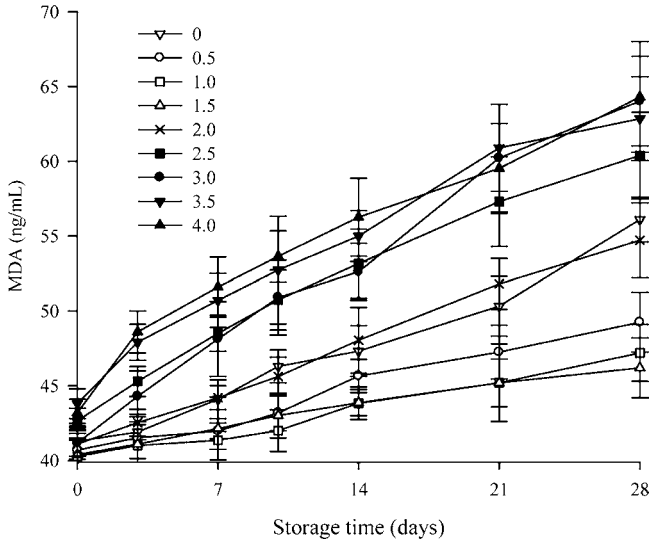

Figure 7. Oxidative stability of bare and decorated liposomes as a function of chitosan concentration during storage at 4 °C. Lipid oxidation was monitored by measuring the malonaldehyde (MDA) value. Each point represents the mean value ± standard deviation (n = 3).

oxidation during storage, which was due to their unsaturated and easily oxidized fatty acids. To the contrary, chitosan decoration ranging from 0.5 to 1.5 mg/mL efficiently suppressed lipid oxidation, except for a slight increase from 14 days. This effect was highly concentration dependent; the more decorated the chitosans were, the more pronounced was their inhibition ability against oxidation. Similar results were observed in a previous study,[47] where the explanation was that the coated layer of chitosan hindered oxygen away from the lipid−water interface by the dense mesh covering on liposomal surface. In the case of liposomes decorated with chitosans of high concentration, the serious lipid oxidation was found even during initial storage, and the MDA values were even higher than those of bare liposomes. It was clear that the high permeability was the result of the damaged integrity of the membrane followed by the penetration of much oxygen. Combined with the variation of membrane fluidity and Raman spectra, the formation of chitosan coils might be the reason for this result, as discussed below.

dx.doi.org/10.1021/jf401556u | J. Agric. Food Chem. 2013, 61, 6901−6910

Chitosan Conformations and Their Influences on Liposome Properties. Having in mind the above consideration, we concluded that there were at least four types of interactions between chitosan and liposomes, which are discussed as follows: (a) At very low concentrations ranging from 0 to 1.0 mg/mL, chitosan was a linear polysaccharide, and the polymer chains were extended when the amino groups were ionized in a good solvent. It was well known that the positive chains adsorbed onto the negative surface of the membrane via electrostatic interaction since the negative charges were neutralized and the net charge of the membrane turned positive, as shown in DLS data. Also, the weak increase of D_z suggested a flat adsorption of chitosan, and the thin chitosan-coated layer was around 10 nm (Figure 5), similar to the manner of adsorption in a previous study.[6] Through this adsorption, not only the integrity of lipid bilayers was maintained but also their physicochemical properties were improved, including the decrease of membrane fluidity, enhancement of the longitudinal order of the bilayer, and inhibition of lipid oxidation. Obviously, these stabilizing effects were attributed to the dense mesh covering of chitosan on the liposomal surface. Actually, the positive influences of the polyelectrolyte-coated layer have also been reported in the literature, such as the stability against salt and pH shocks,[5] thermal properties,[20] drug controlled release,[3] and targeting *in vivo*.[10]

(b) From 1.0 to 1.5 mg/mL, the self-aggregation behavior of chitosan took place, and chains began crimping. Note that the crimping of the chain was accompanied by the formation of hydrophobic microareas (Figures 1 and 2). This phenomenon raised our interest because little research on the interactions between chitosan and liposome involved these hydrophobic microareas. Thus, one question is whether the hydrophobic interaction involved in the chitosan−liposome system and how. Herein, the DLS data might indirectly prove the involvement of hydrophobic interaction since the ζ potential only slightly increased from 1.0 mg/mL, while D_z continued to increase (Figure 5). It indicated that the adsorption of the crimped chain was controlled by both electrostatic and hydrophobic interactions. A previous study also suggested the accommodation of chitosan in the lipid monolayers possibly through hydrophobic interactions.[7] Fluorescence and Raman spectra demonstrated that the incorporation of a hydrophobic group of crimped chains into the lipid bilayer endowed the membrane with less fluidizing properties followed by the enhancement of lipid longitudinal order. The stabilizing role of the hydrophobic interaction may be explained by the conclusion of previous studies,[48] showing that the involvement of hydrophobic interaction promoted the physical adsorption and deposition of chitosan on membrane. The more significant inhibition to lipid oxidation tended to confirm the stronger physical covering of crimped chains (Figure 7). Another important phenomenon has to be mentioned in the polymer−liposome interactions, namely, lipid "flip−flop", suggesting that amphiphilic polymers with hydrophobic blocks may perturb the cooperative packing of lipid molecules throughout the bilayer.[49] For our case, however, the "flippase" activity of chitosan seemed so weak due to its poor hydrophobicity from 1.0 to 1.5 mg/mL that flip−flop may be indistinguishable.

(c) Once the self-aggregation was intensified above 1.5 mg/mL chitosan concentration, plenty of irregular coils and packed coils were generated. It was clear that the presence of coils was not in favor of the flat adsorption of chitosan on the charged liposome surface due to the steric hindrance.[6] According to the practically constant values of ζ potential, it seemed that hydrophobic interaction was a strong driving force of their interactions. As mentioned above, the increase of hydrophobicity indicated a stronger activity of the lipid flip−flop; thus, the hypothesis was given that the adsorption of chitosan hydrophobic blocks accelerated the lipid flip−flop, resulted in irreversible structure arrangement in the liposomal membrane, and subsequently caused some "edge defects" in the lipid bilayer. This, in turn, might be the reason for the destabilizing effects of chitosan on membrane dynamics and structural properties, as shown by fluorescence and Raman spectra. Another reason for this destabilization may be related to the polymeric surfactant property of chitosan. One proposed fact was that the interactions involved the permeation of coils into the lipid bilayer rather than flat adsorption. The damage of membrane integrity based on our oxidation measurements seemed to support coil permeation. This rationale was also based on the data of surface pressure−area isotherms reported by the group of Pavinatto,[13] concluding that chitosan moieties can penetrate among phospholipid chains at large phospholipid areas per molecules (or low surface pressures). If stabilizing the liposome was the aim of chitosan decoration, high decorated concentrations should not be preferred, considering the probably negative properties of this damaged membrane (for example, enhanced permeability of drug and nutraceutical in delivery systems).

(d) At very high concentrations (>2 mg/mL), excessive coils of chitosan were packed. Particle diameter decreased, and two volume peaks appeared (Figure 6). This observation implied that vesicles may undergo a certain degree of disruption by the permeation of excessive irregular and packed coils. As described in section c, chitosan could display strong properties as a polymeric surfactant. In other words, the disruption process induced by chitosan was similar to the traditional micellar solubilization of low-molecular weight surfactants. Besides, it was believed that the lipid flip−flop resulting from polymer permeation exerted pronounced effects on the disruption behavior of liposomes, as emphasized in earlier studies.[49] Due to the potential toxicity and systemic adverse effect resulting from the lipid bilayer membrane disruption, a compromise of chitosan concentrations should be found in the design of polymer decorated liposomes as drug and nutraceutical delivery systems.

As a result of the differences among polyelectrolyte conformations, the binding of a polyelectrolyte to the lipid bilayer membrane (or liposomes) may perturb the bilayer structure and induce three phenomena: fusion, aggregation, or disruption. Some polymers can create a physical barrier on the membrane surface through electrostatic attraction that inhibited fusion and aggregation, while others involved permeation into the lipid bilayer inducing vesicle disruption through the interaction of their hydrophobic blocks with hydrocarbon chains of the lipid bilayer. A general conclusion was given that these different effects were related to polyelectrolyte structure, fraction of charged lipids in the membrane, vesicle phase, and ionic strength of solution.[19] As a few studies have described, our study introduced a typical polymer surfactant (chitosan) and revealed its influence, that is, its ability to disrupt the lipid bilayer membrane, which probably complements the polyelectrolyte conformational dependence of liposome properties.

AUTHOR INFORMATION

Corresponding Author

*Tel: 86-510-85884496. Fax: 86-510-85884496. E-mail: sqxia2006@hotmail.com.

Funding

This research was financially supported by projects of the National Natural Science Foundation for Young Scholars of China (31000815) and the National 125 Program of China (2012BAD33B05).

Notes

The authors declare no competing financial interest.

REFERENCES

(1) Gonnet, M.; Lethuaut, L.; Boury, F. New trends in encapsulation of liposoluble vitamins. *J. Controlled Release* **2010**, *146*, 276−290.

(2) Zucker, D.; Marcus, D.; Barenholz, Y.; Goldblum, A. Liposome drugs' loading efficiency: A working model based on loading conditions and drug's physicochemical properties. *J. Controlled Release* **2009**, *139*, 73−80.

(3) Takeuchi, H.; Kojima, H.; Yamamoto, H.; Kawashima, Y. Evaluation of circulation profiles of liposomes coated with hydrophilic polymers having different molecular weights in rats. *J. Controlled Release* **2001**, *75*, 83−91.

(4) Rinaudo, M. Chitin and chitosan: Properties and applications. *Prog. Polym. Sci.* **2006**, *31*, 603−632.

(5) Quemeneur, F.; Rammal, A.; Rinaudo, M.; Pépin-Donat, B. Large and giant vesicles "decorated" with chitosan: Effects of pH, salt or glucose stress, and surface adhesion. *Biomacromolecules* **2007**, *8*, 2512−2519.

(6) Mertins, O.; Dimova, R. Binding of chitosan to phospholipid vesicles studied with isothermal titration calorimetry. *Langmuir* **2011**, *27*, 5506−5515.

(7) Wydro, P.; Krajewska, B.; Hąc-Wydro, K. Chitosan as a lipid binder: A Langmuir monolayer study of chitosan−lipid interactions. *Biomacromolecules* **2007**, *8*, 2611−2617.

(8) Quemeneur, F.; Rinaudo, M.; Pépin-Donat, B. Influence of polyelectrolyte chemical structure on their interaction with lipid membrane of zwitterionic liposomes. *Biomacromolecules* **2008**, *9*, 2237−2243.

(9) Quemeneur, F.; Rinaudo, M.; Maret, G.; Pepin-Donat, B. Decoration of lipid vesicles by polyelectrolytes: mechanism and structure. *Soft Matter* **2010**, *6*, 4471−4481.

(10) Takeuchi, H.; Matsui, Y.; Yamamoto, H.; Kawashima, Y. Mucoadhesive properties of Carbopol or chitosan-coated liposomes and their effectiveness in the oral administration of calcitonin to rats. *J. Controlled Release* **2003**, *86*, 235−242.

(11) Takeuchi, H.; Matsui, Y.; Sugihara, H.; Yamamoto, H.; Kawashima, Y. Effectiveness of submicron-sized, chitosan-coated liposomes in oral administration of peptide drugs. *Int. J. Pharm.* **2005**, *303*, 160−170.

(12) Fang, N.; Chan, V.; Mao, H.-Q.; Leong, K. W. Interactions of phospholipid bilayer with chitosan: Effect of molecular weight and pH. *Biomacromolecules* **2001**, *2*, 1161−1168.

(13) Pavinatto, F. J.; Pavinatto, A.; Caseli, L.; dos Santos, D. S.; Nobre, T. M.; Zaniquelli, M. E. D.; Oliveira, O. N. Interaction of chitosan with cell membrane models at the air−water interface. *Biomacromolecules* **2007**, *8*, 1633−1640.

(14) Thanou, M.; Verhoef, J. C.; Junginger, H. E. Oral drug absorption enhancement by chitosan and its derivatives. *Adv. Drug Delivery Rev.* **2001**, *52*, 117−126.

(15) Guo, J.; Ping, Q.; Jiang, G.; Huang, L.; Tong, Y. Chitosan-coated liposomes: characterization and interaction with leuprolide. *Int. J. Pharm.* **2003**, *260*, 167−173.

(16) Tommy, N.; Yulia, S.; Björn, L. Formation of polyelectrolyte-surfactant complexes on surfaces. *Sci. Adv. J. Colloid Interface Sci.* **2006**, *123−26*, 105−123.

(17) Yaroslavov, A. A.; Sybachin, A. V.; Kesselman, E.; Schmidt, J.; Talmon, Y.; Rizvi, S. A. A.; Menger, F. M. Liposome fusion rates depend upon the conformation of polycation catalysts. *J. Am. Chem. Soc.* **2011**, *133*, 2881−2883.

(18) Osanai, S.; Nakamura, K. Effects of complexation between liposome and poly(malic acid) on aggregation and leakage behaviour. *Biomaterials* **2000**, *21*, 867−876.

(19) Kabanov, V. A.; Yaroslavov, A. A. What happens to negatively charged lipid vesicles upon interacting with polycation species? *J. Controlled Release* **2002**, *78*, 267−271.

(20) Yaroslavov, A. A.; Efimova, A. A.; Lobyshev, V. I.; Kabanov, V. A. Reversibility of structural rearrangements in the negative vesicular membrane upon electrostatic adsorption/desorption of the polycation. *Biochim. Biophys. Acta, Biomembr.* **2002**, *1560*, 14−24.

(21) Philippova, O. E.; Volkov, E. V.; Sitnikova, N. L.; Khokhlov, A. R.; Desbrieres, J.; Rinaudo, M. Two types of hydrophobic aggregates in aqueous solutions of chitosan and its hydrophobic derivative. *Biomacromolecules* **2001**, *2*, 483−490.

(22) Pepić, I.; Filipović-Grčić, J.; Jalšenjak, I. Interactions in a nonionic surfactant and chitosan mixtures. *Colloids Surf., A* **2008**, *327*, 95−102.

(23) Ai, H.; Jones, S.; Lvov, Y. Biomedical applications of electrostatic layer-by-layer nano-assembly of polymers, enzymes, and nanoparticles. *Cell Biochem. Biophys.* **2003**, *39*, 23−43.

(24) Pavinatto, A.; Pavinatto, F. J.; Barros-Timmons, A.; Oliveira, O. N. Electrostatic interactions are not sufficient to account for chitosan bioactivity. *ACS Appl. Mater. Interfaces* **2009**, *2*, 246−251.

(25) Pavinatto, F. J.; Caseli, L.; Pavinatto, A.; dos Santos, D. S.; Nobre, T. M.; Zaniquelli, M. E. D.; Silva, H. S.; Miranda, P. B.; de Oliveira, O. N. Probing chitosan and phospholipid interactions using Langmuir and Langmuir−Blodgett films as cell membrane models. *Langmuir* **2007**, *23*, 7666−7671.

(26) Xia, S.; Xu, S.; Zhang, X.; Zhong, F. Effect of coenzyme Q10 incorporation on the characteristics of nanoliposomes. *J. Phys. Chem. B* **2007**, *111*, 2200−2207.

(27) Henriksen, I.; Våagen, S. R.; Sande, S. A.; Smistad, G.; Karlsen, J. Interactions between liposomes and chitosan II: Effect of selected parameters on aggregation and leakage. *Int. J. Pharm.* **1997**, *146*, 193−203.

(28) Xia, S.; Xu, S.; Zhang, X. Optimization in the preparation of coenzyme Q10 nanoliposomes. *J. Agric. Food Chem.* **2006**, *54*, 6358−6366.

(29) Shinitzky, M.; Barenholz, Y. Fluidity parameters of lipid regions determined by fluorescence polarization. *Biochim. Biophys. Acta* **1978**, *515*, 367−394.

(30) Fukui, Y.; Fujimoto, K. The preparation of sugar polymer-coated nanocapsules by the layer-by-layer deposition on the liposome. *Langmuir* **2009**, *25*, 10020−10025.

(31) Miceli, N.; Trovato, A.; Dugo, P.; Cacciola, F.; Donato, P.; Marino, A.; Bellinghieri, V.; La Barbera, T. M.; Güvenç, A.; Taviano, M. F. Comparative analysis of flavonoid profile, antioxidant and antimicrobial activity of the berries of *Juniperus communis* L. var. communis and *Juniperus communis* L. var. saxatilis Pall. from Turkey. *J. Agric. Food Chem.* **2009**, *57*, 6570−6577.

(32) Schatz, C.; Viton, C.; Delair, T.; Pichot, C.; Domard, A. Typical physicochemical behaviors of chitosan in aqueous solution. *Biomacromolecules* **2003**, *4*, 641−648.

(33) Amiji, M. M. Pyrene fluorescence study of chitosan self-association in aqueous solution. *Carbohydr. Polym.* **1995**, *26*, 211−213.

(34) Gao, Q. U. N.; Wan, A. Effects of molecular weight, degree of acetylation and ionic strength on surface tension of chitosan in dilute solution. *Carbohydr. Polym.* **2006**, *64*, 29−36.

(35) Pavinatto, F. J.; Caseli, L.; Oliveira, O. N. Chitosan in Nanostructured Thin Films. *Biomacromolecules* **2010**, *11*, 1897−1908.

(36) Jemiola-Rzeminska, M.; Kruk, J.; Skowronek, M.; Strzalka, K. Location of ubiquinone homologues in liposome membranes studied by fluorescence anisotropy of diphenyl-hexatriene and trimethylammonium-diphenyl-hexatriene. *Chem. Phys. Lipids* **1996**, *79*, 55−63.

(37) Li, H. T.; Wang, M. L.; Zhang, Y. Y.; He, B. L. Aggregation behavior of chitosan in dilute aqueous solution. *Chin. J. Appl. Chem.* **2004**, *21*, 159−163.
(38) Hincha, D. K. Effects of α-tocopherol (vitamin E) on the stability and lipid dynamics of model membranes mimicking the lipid composition of plant chloroplast membranes. *FEBS Lett.* **2008**, *582*, 3687−3692.
(39) Hauser, H.; Phillips, M. C.; Levine, B. A.; Williams, R. J. P. Conformation of the lecithin polar group in charged vesicles. *Nature* **1976**, *261*, 390−394.
(40) Mendelsohn, R.; Sunder, S.; Bernstein, H. J. Structural studies of biological membranes and related model systems by raman spectroscopy: Sphingomyelin and 1,2-dilauroyl phosphatidylethanolamine. *Biochim. Biophys. Acta, Biomembr.* **1975**, *413*, 329−340.
(41) Pink, D. A.; Green, T. J.; Chapman, D. Raman scattering in bilayers of saturated phosphatidylcholines. Experiment and theory. *Biochemistry* **1980**, *19*, 349−356.
(42) Mendelsohn, R.; Van Holten, R. W. Zeaxanthin ([3R,3′R]-beta, beta-carotene-3−3′diol) as a resonance Raman and visible absorption probe of membrane structure. *Biophys. J.* **1979**, *27*, 221−235.
(43) Li, X.-M.; Zhao, B.; Zhao, D.-Q.; Ni, J.-Z.; Wu, Y.; Xu, W.-Q. Interaction of La3+ and cholesterol with dipalmitoylphosphatidylglycerol bilayers by FT-Raman spectroscopy. *Thin Solid Films* **1996**, *284*−*285*, 762−764.
(44) Gaber, B. P.; Peticolas, W. L. On the quantitative interpretation of biomembrane structure by Raman spectroscopy. *Biochim. Biophys. Acta, Biomembr.* **1977**, *465*, 260−274.
(45) Chu, B.; Wang, Z.; Yu, J. Dynamic light scattering study of internal motions of polymer coils in dilute solution. *Macromolecules* **1991**, *24*, 6832−6838.
(46) Asayama, K.; Aramaki, Y.; Yoshida, T.; Tsuchiya, S. Permeability changes by peroxidation of unsaturated liposomes with ascorbic acid/Fe2+. *J. Liposome Res.* **1992**, *2*, 275−287.
(47) Panya, A.; Laguerre, M.; Lecomte, J.; Villeneuve, P.; Weiss, J.; McClements, D. J.; Decker, E. A. Effects of chitosan and rosmarinate esters on the physical and oxidative stability of liposomes. *J. Agric. Food Chem.* **2010**, *58*, 5679−5684.
(48) Mertins, O.; da Silveira, N. P.; Pohlmann, A. R.; Schröder, A. P.; Marques, C. M. Electroformation of giant vesicles from an inverse phase precursor. *Biophys. J.* **2009**, *96*, 2719−2726.
(49) Yaroslavov, A. A.; Melik-Nubarov, N. S.; Menger, F. M. Polymer-induced flip-flop in biomembranes. *Acc. Chem. Res.* **2006**, *39*, 702−710.